Dynamics of growing interfaces from the simulation of unstable flow in random media

M. Ferer
Department of Physics, West Virginia University, P.O. Box 6315, Morgantown, West Virginia 26506-6315

Duane H. Smith
U.S. Department of Energy, Morgantown Energy Technology Center, Morgantown, West Virginia 26507-0880

(Received 13 December 1993)

Viscous fingering in random porous media is encountered in many applications of two-phase flow, where the interface is unstable because the ratio of the viscosity of the displaced fluid to that of the injected fluid is large. In these applications, including enhanced oil recovery, characterization of the width of the interface is an important concern. In the limit of stable flow, the interfacial width had been found to grow as $w \approx t^{\beta}$, where $\beta \approx 0.66$, approximately independent of capillary number. To study the same behavior for the unstable case, we have simulated flow in two-dimensional random porous media using a standard model with different viscosity ratios and zero capillary pressure. When the injected fluid has zero viscosity, viscosity ratio $M=\infty$, the interfacial width has the expected self-similar diffusion-limited-aggregation-like behavior. For smaller viscosity ratios, the flow is self-affine with $\beta=0.66\pm0.04$, which is the same value that had been observed in studies of stable flow. Furthermore, the crossover from self-similar fractal flow to self-affine fractal flow is observed to scale with the same "characteristic" time, $\tau=M^{0.17}$, that had been found to scale the average interface position. This "fractal" scaling of the crossover leads to definite predictions about the viscosity-ratio dependence of the amplitudes associated with interfacial position and interfacial width.

PACS number(s): 68.10.−m, 47.55.Mh, 03.40.Gc

I. INTRODUCTION

The structure of driven interfaces has been the subject of extensive study during the past decade [1]. The marginally stable development of an initially smooth surface into a generically rough surface can be described through the scaling of the interfacial width, W, with time t and lateral size L. This scaling function takes the form

$$W = t^{\beta} f(t/L^{\alpha/\beta}) , \tag{1}$$

where α is the roughness exponent since $W \approx L^{\alpha}$ when $t \gg L^{\alpha/\beta}$. β is often called the dynamical exponent since $W \approx t^{\beta}$ when $t \ll L^{\alpha/\beta}$, (some authors call $z=\alpha/\beta$ the dynamical exponent, in which case they name β the "early-time" exponent). This marginally stable development of a rough interface has been observed in a broad class of growth phenomena including stable flow in porous media [2–4], surface deposition [5,6] directed polymers and bacteria growth [7], in addition to several other growth problems like the roughness associated with the wetting or the burning of paper [8,9]. Simulations of wetting invasion show similar behavior using an invasion percolation model where capillary forces dominate [10].

Unambiguous analytic results in two dimensions, based on the Kardar-Parisi-Zhang (KPZ) equation [11], gave values of the exponents $\alpha=\frac{1}{2}$ and $\beta=\frac{1}{3}$ [11], which satisfy the scaling identity

$$\alpha+z=\alpha+\alpha/\beta=2 . \tag{2}$$

However, the values from the experiments on two-dimensional systems, discussed above, all indicate larger values of the indices, e.g., $\alpha \approx 0.68 \rightarrow 0.85$, with most of the values clustering around $\alpha \approx 0.8$ and $\beta \approx 0.67$. A recent measurement of both the dynamic index and the roughness index from a Hele-Shaw experiment determined that $\beta \approx 0.65$ and $\alpha \approx 0.81$, which values satisfy the scaling identity $\alpha+z=2$ [2]. In an attempt to explain the discrepancy between the experiments and the seemingly general theory. Zhang postulated that "rare" events can scale to give a power-law tail to the noise distribution in the KPZ equation which would lead to nonuniversal dynamics and roughening exponents depending upon the exponent μ in the power-law tail [e.g., in d dimensions, $\alpha=(d+2)/(\mu+1)$ for $\mu_c<\mu<d+2$] [12]. Subsequent theoretical work supports these predictions [13,14]. Although this work may explain why experimental values are so different from the first results of the KPZ equation, it is still somewhat surprising that such a wide range of experimental systems can be described by nearly "universal" values of the indices α and β. Is the power-law exponent μ also universal, and if so why? However, recent work studying the crossover from KPZ growth to power-law noise growth showed that logarithmic corrections near the crossover seem to smooth the variation in the roughness exponent [14].

In much of the previous work there has been a single-valued interface $h(x,t)$ at a given lateral position x, i.e., there are no significant overhangs, as one observes in diffusion-limited aggregation. Furthermore, many of the systems theoretically and experimentally have a pinning mechanism, e.g., capillary pressure [3,4,10,15,16], which could be the source of the power-law noise necessary for the KPZ equation to give the experimentally observed in-

dices. It is intriguing that recent work on fracturing in nearly two-dimensional solids [17], where the pinning-depinning is manifest, shows that the fracture width scales with nearly the same roughness exponent, $w \approx L^{0.87}$, as the growth fronts discussed above.

We have simulated a physically realistic model of miscible two-phase, Poiseuille flow in porous media which differs from the above systems in three respects: (i) our simulations study the "unstable" flow limit for viscosity ratios $M > 1$ up to the $M \to \infty$ limit, at which limit the flow is modeled by diffusion-limited aggregation (DLA); (ii) there is no obvious pinning mechanism because Poiseuille flow is valid in the limit of infinite capillary number (zero capillary pressure); and (iii) there is not a single-valued interfacial position, $h(x,t)$, because of overhangs and droplet breakoff as can be seen in Fig. 1. In earlier papers [18,19], we have shown that the flow in this system crosses over from DLA-like mass fractal [(mass) $\approx$ (time) $\approx$ (size)^{D_f}] for $M = \infty$ to a compact object [(mass) $\approx$ (time) $\approx$ (size)^d] for finite M where D_f is the fractal dimension and d is the Euclidean dimension. This crossover was shown to occur at length scale l which increases with the ratio of the fluid viscosities as $l \approx M^{0.24}$, so that in the limit of infinite viscosity ratio (where the injected fluid has zero viscosity) the flow has the expected DLA-like behavior at all length scales [18].

In this paper, we characterize the interfacial width associated with the viscous fingering in this model of unstable flow, which is relevant to a wide range of applications including enhanced oil recovery. In the DLA limit the flow patterns should be self-similar, so that all lengths should scale in the same way with time (mass of the injected fluid), so that the width w and the average interfacial position $\langle h \rangle$ scale as

$$\langle h \rangle \approx w \approx t^{1+\varepsilon} , \tag{3}$$

where $1+\varepsilon \equiv 1/(D_f - 1) \approx 1.4$ for DLA growth in the short, wide rectangular systems shown in Fig. 1 [18]. After the flow has crossed over to the compact regime so that $\langle h \rangle \approx t$, the interface is still rough with $w \approx t^{\beta}$, characteristic of self-affine fractal patterns. Analyzing the interfacial width, we will characterize the behavior of the width in both the self-similar and self-affine limits, as well as the crossover between the two limits.

II. DESCRIPTION OF THE MODEL

In modeling two-phase, Poiseuille flow in porous media, we have used a simple, standard model which is as physically realistic as possible; a detailed discussion is presented in Ref. [18]. We assumed a variant of the standard square lattice model of homogeneous two-dimensional porous media [20,21], and [22] in which the pore bodies, at the sites of a square lattice, all have unit

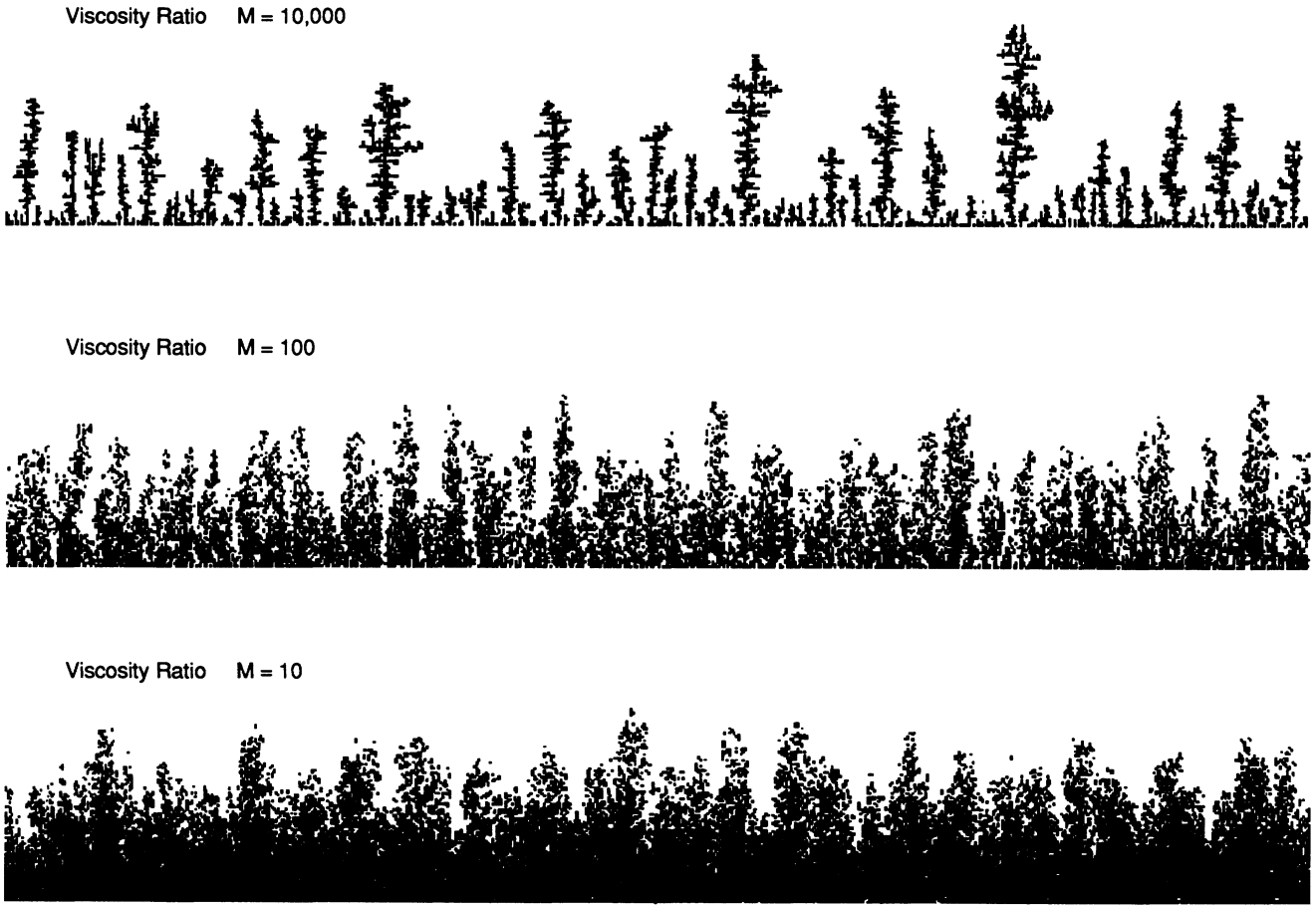

FIG. 1. Near-breakthrough flow patterns for three viscosity ratios.

volume, but the cross-sectional area of each pore throat is randomly chosen from a uniform distribution. This distribution is known to give random, fractal flow for infinite viscosity ratio [22]. Knowing the conductances from the geometry of the porous medium and the location of the interface, we then use a slight modification of the standard Gauss-Seidel iteration of the discrete Laplace equation until the residual is less than 10^{-5}. This upper bound on the residual and the flow rules, to be described shortly, were found to satisfy total fluid conservation to within 0.5%, even after 1400 time steps. Knowing the conductance and the pressure drops across the throats enables us to determine the flow rate for each throat. A straightforward deterministic procedure is then used to advance the interface through a short time Δt. Although there is zero interfacial tension in Poiseuille flow, there is a well-defined interface in our model flows, because we have assumed negligible dispersion of the two phases. Flow is allowed in every throat; and the deterministic flow velocity is allowed to advance (or retreat) the interface within the pore throat, into its connecting pore body, and through a pore body into its outflow throats. This procedure has the advantage of not suppressing fractal flow [21] as do averaged methods, such as the grid-block procedure [23]. Indeed, earlier variants of this model were used to study fractal flow [21,22,24], and we have verified that the large viscosity-ratio limit of this model does produce the expected DLA-like fractal flows [18]. In this model we have defined time to be proportional to the total injected volume $V_{\rm tot}$, specifically $t=1.3+(V_{\rm tot}/N)$, where N is the number of inlet sites (i.e., lateral width) and the small additive shift of 1.3 arises from the discreteness of the model and only serves to reduce early time curvature in the fractal dimension plots [18]. Since our earlier papers, we have performed additional simulations to improve the statistics for the interfacial width. These additional simulations were performed on porous media which were 96 pore bodies long (in the flow direction) by 640 pore bodies wide; several near-breakthrough patterns from these simulations are showing in Fig. 1. These simulations were performed on the CRAY YMP at the University of Nevada at Las Vegas, with each simulation requiring an average of three hours of CPU time.

III. DYNAMICAL BEHAVIOR OF THE INTERFACE

Figure 1 shows qualitatively how the flow patterns change from a DLA-like limit near the infinite viscosity ratio to self-affine behavior with a compact background and a rough interface at a much smaller viscosity ratio. To characterize this behavior, we have modeled flows for viscosity ratios in the crossover regime $M=10$, 30, 100, and 300, as well as for $M=10\,000$ near the DLA-like limit. To quantify the observed behavior, we have determined the interfacial width w and the time t at each time step during the simulations. For each viscosity ratio, we performed these simulations for a number of different realizations of the model porous medium, and we averaged the output of the different realizations as described in an earlier paper [18]. Figure 2 shows the resulting averaged data for $w/t^{1.4}$ vs t for all the viscosity ratios studied; the standard errors are no larger than the data points. As expected from above, the data for $M=10\,000$ show self-similar DLA-like fractal behavior, Eq. (3) with $w/t^{1.4}\approx$const. For the smaller viscosity ratios, the curves initially follow the constant self-similar fractal behavior, but, beginning with the $M=10$ data, they all break away and approach a straight line of negative slope, characteristic of the rough interfaces $w\approx t^{\beta}$. As with the average position of the interface [18], this breakaway or crossover occurs on a characteristic time scale τ, which increases with the viscosity ratio. Figure 2 shows a well-defined crossover from DLA-like growth ($w/t^{1.4}\approx$const) to eventual self-affine behavior ($w/t^{1.4}\approx t^{\beta-1.4}$) for all relevant viscosity ratios. To determine the value of the dynamical exponent β, we fit the linear portion of the data in Fig. 2, obtaining values of β in the range $0.62<\beta<0.69$. To demonstrate the goodness of the fit, Fig. 3 shows the data for $w/t^{0.66}$ vs t; here, the data initially follow the fractal behavior ($w/t^{0.66}\approx t^{1.4-0.66}$) breaking away at the characteristic crossover time to approach a constant. Since the small viscosity-ratio data are so constant in Fig. 3, we assert that $\beta=0.66\pm0.04$, which is consistent with the least-squares fits above. To well within errors, our result for unstable flow agrees with the experimental determination $\beta\approx0.65$ from the injection of glycerol into air (the extreme stable limit, $M\ll1$) [2].

Our earlier study of the average interfacial position in these edge injection systems showed that a characteristic crossover time $\tau\approx M^{\phi_t}$, where $\phi_t=0.17\pm0.03$, served to scale (i.e., account for the viscosity-ratio dependence of) all the asymptotic data, but that a correction to scaling significantly improved the scaling of the nonasymptotic data [18]. Physically, this correction to scaling, $\Delta=8/M^{0.17}$, represents a viscosity-ratio-dependent shift of the time origin, which does vary relatively little between the viscosity ratios in the crossover regime. In short, the variable $u=\{t+(8/M^{0.17})\}/M^{0.17}$ served to

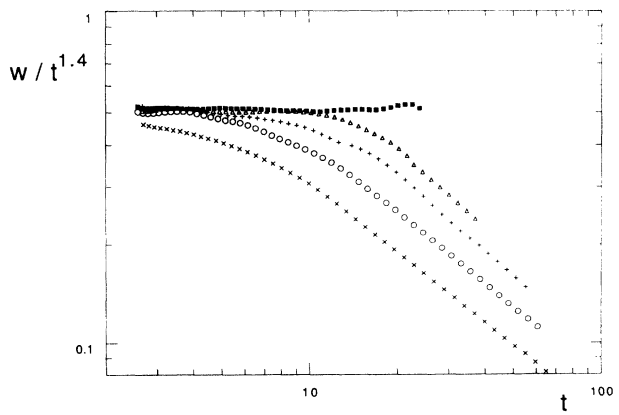

FIG. 2. Plot of the smoothed data for $w/t^{1.4}$ vs t, for viscosity ratios $M=10$ (×), $M=30$ (○), $M=100$ (+), $M=300$ (△), and $M=10\,000$ (■), showing the self-similar fractal character (DLA-like) of the early time flows.

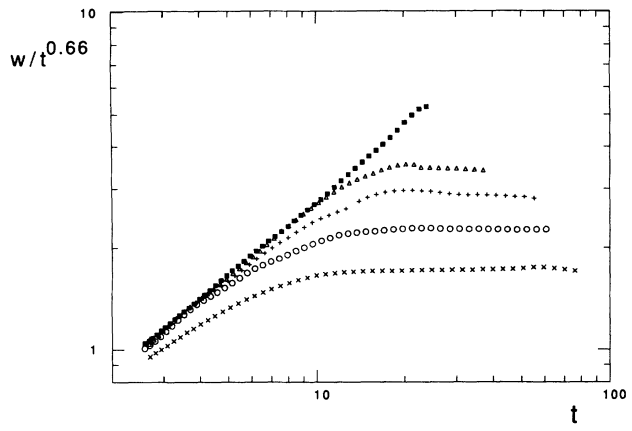

FIG. 3. Plot of the smoothed data for $w/t^{0.66}$ vs t, for viscosity ratios $M=10$ (×), $M=30$ (○), $M=100$ (+), $M=300$ (△), and $M=10000$ (■) showing the self-affine character (with $\beta\approx 0.66$) of the post-crossover flows.

scale the data for average interfacial position. If this variable correctly scales the interfacial position, it seems likely that the same variable should scale the interfacial width, especially since the scaling in the DLA limit should be self-similar. Therefore one expects that interfacial width would scale as

$$w=t^{1/\varepsilon}\Omega\left[\frac{t+\Delta}{\tau}\right], \tag{4}$$

where $1+\varepsilon=1.4\pm0.05$, $\Delta=(8/M^{0.17})$, and $\tau=M^{\phi_t}$, where $\phi_t=0.17\pm0.03$. This scaling expression is tested in Fig. 4, where we have used our data to plot $w/t^{1.4}$ vs $(t+\Delta)/\tau$. The data obey the scaling prediction quite well, supporting the hypothesis that the same crossover scaling should apply to both the interfacial position and width.

The scaling of the interfacial position enabled us to determine the viscosity-ratio dependence of the amplitude describing the linear advance of the interface in the post-crossover regime, $t\gg\tau$; specifically,

$$\langle h\rangle=v(M)t,\quad v(M)\approx v_0M^{\varepsilon\phi_t}, \tag{5}$$

where $\varepsilon\phi_t=0.07\pm0.02$ [18]. Here the scaling of the interfacial width enables us to determine the viscosity-ratio dependence of the amplitude for the self-affine growth of the interfacial width in the post-crossover regime. At large times,

$$\lim_{t\to\infty} w=\omega(M)t^{\beta}, \tag{6a}$$

so that

$$\begin{aligned} t^{1+\varepsilon}\lim_{t\to\infty}\Omega\left[\frac{t+\Delta}{\tau}\right]&=t^{1+\varepsilon}\lim_{t\to\infty}\Omega(t/\tau)\\ &=\omega_0t^{1+\varepsilon}\left[\frac{t}{\tau}\right]^{\beta-(1+\varepsilon)}\\ &=\omega_0(M^{\phi_t})^{-\beta+(1+\varepsilon)}t^{\beta}, \end{aligned} \tag{6b}$$

where the scaling function $\Omega(u)$ must have the right large time dependence $\Omega(u)\approx(u)^{\beta-(1+\varepsilon)}$ to give the t^{β} behavior in the post-crossover limit. This shows that the viscosity-ratio dependence of the interfacial width must be described by an exponent $\phi_t(1+\varepsilon-\beta)=0.126\pm0.035$, which shows a small power-law increase of the interfacial width with increasing viscosity ratio.

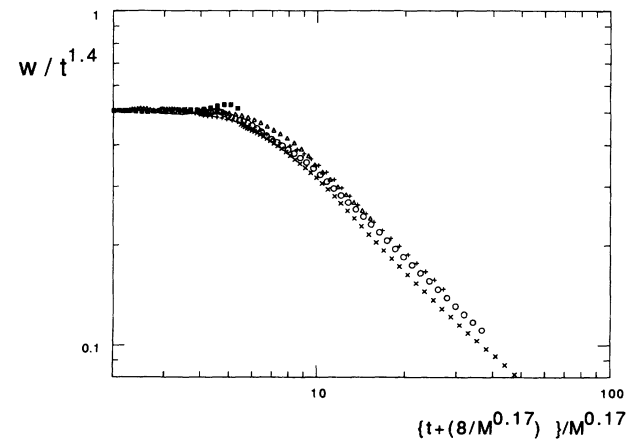

FIG. 4. Scaling plot [Eq. (4)] of the smoothed data for viscosity ratios $M=10$ (×), $M=30$ (○), $M=100$ (+), $M=300$ (△), and $M=10000$ (■).

IV. INTERFACIAL ROUGHNESS

In the experiments on stable systems, there is a well-defined (i.e., single valued) interfacial position so that the "scale" roughness develops from zero at small scales ($L=0$) to the asymptotic t^{β} values for $L\gg t^{\beta/\alpha}$. Because of overhangs and droplet breakoff in our simulations [see Fig. (1)], at any given point x in the lateral direction, one can only define an average interfacial position; and the fluid interface has a finite width at any given point x. Our quantitative definitions of average interfacial position $\langle h\rangle$ and average interfacial width w are discussed in the Appendix. Small-scale or intrinsic widths were also observed in the Eden model [25] and in invasion percolation models [10]. Our interfaces have a large zero-scale width, which is nearly as big as the asymptotic width, i.e., $w(t,L=0)$ is nearly as large as $w(t,L=\infty)$. Figure 5 shows this effect for $M=10$ flows at four post-crossover times; at each time the zero scale width is more than 70% of the asymptotic width. Therefore, scale roughness is much less significant in our simulations of unstable flow, and asymptotic widths are achieved at much smaller L than is the case in the experiments on stable flow where the intrinsic width is zero and "scale" roughness is far more significant. Even so, we are able to estimate that $\alpha\approx0.8$, from the small-scale data ($L<20$). Our estimates for α and β agree with the scaling relation between α and β, Eq. (2), which has proven reliable for other systems. Figure 6 shows the result of attempting to scale the interfacial width using the form in Eq. (1) and our estimates for the values of the indices; the overlap of the data for different times shows that our

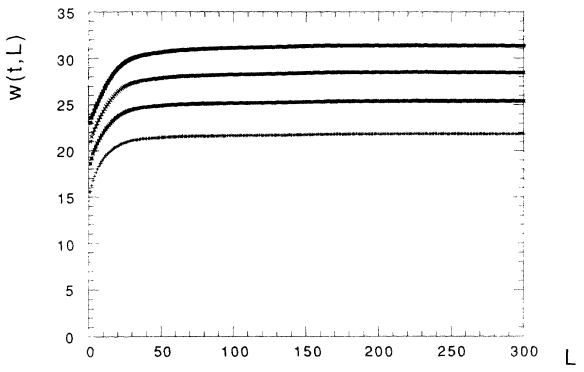

FIG. 5. The scale roughness in $w(t,L)$ for viscosity ratio $M=10$ at times $t=43$ (+), $t=53$ (*), $t=63.5$(×), and $t=74$ (■).

data are consistent with this standard scaling of the interface. The straight line in Fig. 6 has slope 0.8, indicating the reliability of our estimate $\alpha\approx 0.8$.

V. CONCLUSIONS

This work shows that the compact to fractal crossover characterized in our earlier papers [18,19] is actually a crossover from DLA-like self-similar fractal flow at $M=\infty$ to the self-affine flow at finite viscosity ratio. The dynamical and roughness exponents characterizing the development of the interface in our simulations of unstable flow were $\beta=0.66\pm0.04$ and $\alpha=0.80\pm0.03$, where the uncertainty in α was determined from the scaling relation Eq. (2). These are essentially the same values which characterize the well-studied stable flow for a variety of capillary numbers. This is a surprising universality, given the differences between our model [(i) unstable flow, (ii) absence of a pinning mechanism, and (iii) importance of short-scale width] and the other systems studied; it is especially surprising since the theory (modified KPZ equation) predicts that the indices should depend on a parameter, the power characterizing the small probability noise.

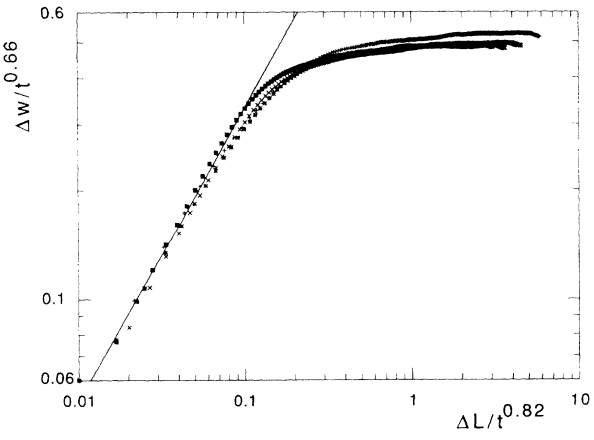

FIG. 6. The scaling [Eqs. (1) and (2)] of $w(t,L)$ for viscosity ratio $M=10$ at times $t=43$ (+), $t=53$ (*), $t=63.5$(×), and $t=74$ (■). The straight line has slope 0.8 showing the reliability of our estimate $\alpha\approx 0.8$.

The crossover of the interfacial width from self-similar DLA-like behavior at infinite viscosity ratio to self-affine (compact) behavior scales with the same characteristic time, $\tau=M^{\phi_t}$ ($\phi_t=0.17\pm0.03$) that was shown to scale the interfacial position in our earlier work [18]. This fractal scaling of the interfacial position and width enabled us to determine the viscosity-ratio dependence of the amplitudes in the self-affine post-crossover flow

$$\lim_{t\to\infty}\langle h\rangle = v(M)t,\quad v(M)\approx v_0 M^{\varepsilon\phi_t},$$
$$\lim_{t\to\infty} w=\omega(M)t^{\beta},\quad \omega(M)\approx\omega_0(M^{\phi_t})^{1+\varepsilon-\beta}, \tag{7}$$

where $\varepsilon\phi_t=0.07\pm0.02$ and $\phi_t(1+\varepsilon-\beta)=0.126\pm0.035$, so that both the interfacial position and the interfacial width are described by a small power-law increase with viscosity ratio.

Because of the surprising universality of interfacial scaling exponents, we are studying the noise associated with the flow in order to understand any similarities or differences between the noise distributions in our model with those in systems with pinning mechanisms.

ACKNOWLEDGMENTS

M.F. gratefully acknowledges the support of the Fossil Energy Program, U.S. Department of Energy.

APPENDIX: DETERMINING THE WIDTH OF A LOCALLY ROUGH INTERFACE

The interfaces for unstable flow demonstrate the short-scale roughness, as discussed in the text. Because of overhangs and droplet breakoff resulting from fluctuations in crossflow, there is not one well-defined interfacial height h at a given position x along the direction perpendicular to flow. This presents more of an ambiguity in locating the interface and determining its width than one usually encounters in the standard, driven interface problems where the width can be unambiguously defined $W^2=\langle[h(x)-\langle h\rangle]^2\rangle$. However, judicious use of the first and second moments of the position of the injected fluid allow a determination of the interfacial height h_0 and its width W, which correctly reproduce results for general density profiles. The following arguments are intended to justify our definition of the width in terms of these first and second moments.

For the time being, let us restrict ourselves to a flow pattern with a Gaussian interface. Averaging the density of injected fluid over some length L of the direction perpendicular to the average flow, one finds a density $\rho(y)$, which we assume to have a Gaussian profile for the present discussion. That is, the density of injected fluid has the form shown in Fig. 7, where the derivative of the density is the Gaussian

$$-\rho'(y)=\rho_0\left[\frac{\pi}{w}\right]^{1/2}\exp^{-(y-h_0)^2/w^2}. \tag{A1}$$

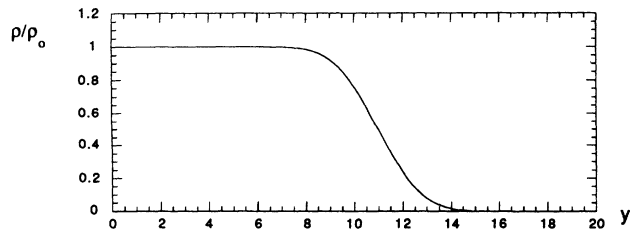

FIG. 7. Gaussian saturation profile.

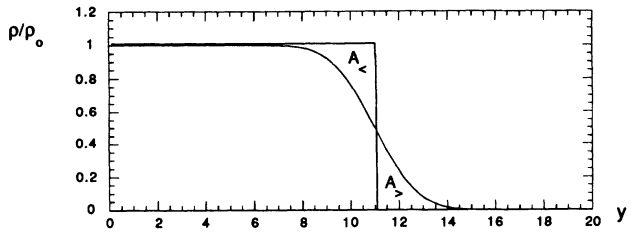

FIG. 9. General saturation profile.

Clearly, this Gaussian interface is centered at the height h_0 with width w, and the integral of Eq. (A1) reproduces the average density profile shown in Fig. 7. The moments $\mu_n = \int_0^\infty y^n \rho(y)dy$ of this average density profile can be determined exactly, and one finds

$$m = \mu_0 = \rho_0 h_0 ,$$
$$\langle y \rangle = \mu_1/\mu_0 = \left[\frac{h_0}{2} + \frac{w^2}{4h_0} \right] , \tag{A2}$$
$$\langle y^2 \rangle = \mu_2/\mu_0 = \left[\frac{h_0^2}{3} + \frac{w^2}{2} \right] .$$

Therefore, the width of the interface can be determined from the appropriate fluctuation in the average position

$$W^2 = 3\langle y^2 \rangle - 4\langle y \rangle^2 = \tfrac{1}{2} w^2 \left[1 - \frac{1}{2} \left[\frac{w}{h_0} \right]^2 \right] , \tag{A3}$$

where the "correction" term $(w/h_0)^2$ is a constant for self similar fractals and vanishes as $t^{-2+2\beta}$ for self-affine fractals. Therefore, although both moments have a leading term depending on the interfacial position h_0, the appropriate fluctuation Eq. (A3) removes this dependence leaving the dependence on interfacial width as the leading dependence.

It is possible to justify the same expression for the width, i.e., Eq. (A3) for a general density profile, like the one in Fig. 8, which shows the saturation from our simulations of flow for viscosity ratio $M = 10$, at a time just prior to breakthrough. Figure 9 shows a general density profile, overlaying a sharp interface; Fig. 10 shows the negative of the derivative of the density profile. We choose the interface position x_0 so that the area under the density profile equals the area under the sharp interface overlay. This requires that the two areas A must be equal: $A_< = A_>$, and that the first moment of the derivative of the density profile (Fig. 10) be zero. Therefore, integrating by parts, one can evaluate the zeroth moment of the density profile, which equals the zeroth moment of the sharp interface profile with our choice for h_0:

$$m = \mu_0 = \int_0^\infty y\rho'(y)dy$$
$$= h_0 \int_{-\infty}^\infty \rho'(u)du + \int_{-\infty}^\infty u\rho'(u)du = \rho_0 h_0 , \tag{A4}$$

where $u = y - h_0$, and the final equality follows because the first integral must be ρ_0 and the second must be zero because of our choice of h_0. Integrating the first moment by parts, one finds

$$\mu_1 = \int_0^\infty \frac{y^2}{2}\rho'(y)dy$$
$$= \frac{h_0^2}{2} \int_{-\infty}^\infty \rho'(u)du + h_0 \int_{-\infty}^\infty u\rho'(u)du$$
$$+ \int_{-\infty}^\infty \frac{u^2}{2}\rho'(u)du . \tag{A5}$$

As above, the first and second integrals have the values ρ_0 and zero, respectively, because the third integral is a measure of the mean square of width of the interface (i.e., the distribution shown in Fig. 10), we will define it to be $\rho_0(w^2/2)$. Therefore the average position is the same as in Eq. (A2). Integrating the second moment by parts, we find

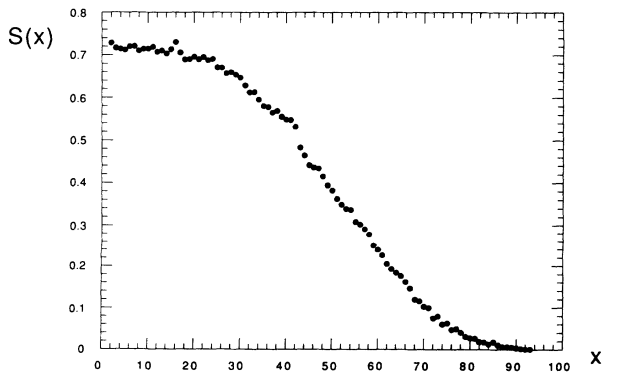

FIG. 8. Near-breakthrough saturation profile from simulations of flow for viscosity ratio $M = 10$.

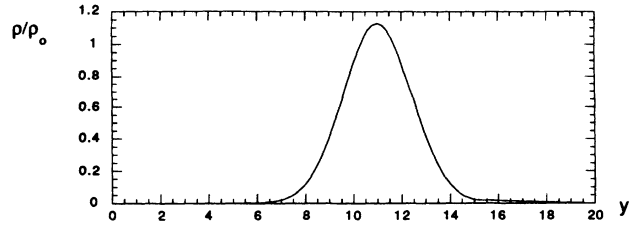

FIG. 10. $-\rho'$ is the negative of the derivative of the general saturation profile.

$$\mu_2=\int_0^\infty \frac{y^3}{3}\rho'(y)dy$$
$$=\frac{h_0^3}{3}\int_{-\infty}^{\infty}\rho'(u)du+h_0^2\int_{-\infty}^{\infty}u\rho'(u)du$$
$$+h_0\int_{-\infty}^{\infty}\frac{u^2}{2}\rho'(u)du+\int_{-\infty}^{\infty}\frac{u^3}{3}\rho'(u)du\ . \quad \text{(A6)}$$

The first three integrals have the values ρ_0, zero, and $w^2/2$, respectively, as discussed above for the first moment. If $\rho'(y)$ is a symmetric function about the average interface position h_0, then the fourth integral will be zero; even if the interface is skewed and $\rho'(y)$ is not symmetric when compared with the other terms, the fourth integral will be a small correction proportional to the amount of asymmetry in the interface. Therefore to a good approximation, $\langle y^2\rangle=\mu_2/\mu_0$ will have the same form as in Eq. (A2).

Obviously there is a difference between the integrals evaluated above and the corresponding sums we actually perform in calculating the moments for our discrete lattices, i.e., the sum of a function only equals the integral in the limit of infinitesimal step size. These sums can be performed exactly for density profile with a sharp interface [pistonlike flow where $\rho(y)=\rho_0$ for $y\le h_0$ for integrals y and h_0]; obviously this density profile has a zero interfacial width $w=0$. Determining the moments from the appropriate sums,

$$\mu_n=\sum_{y=1}^{h_0} y^n\rho_0\ , \quad \text{(A7)}$$

one finds

$$\langle y\rangle_d=\left[\frac{h_0}{2}+\frac{1}{2}\right] \quad \text{(A8a)}$$

and

$$\langle y^2\rangle_d=\left[\frac{h_0^2}{3}+\frac{h_0}{2}+\frac{1}{6}\right]\ . \quad \text{(A8b)}$$

If one uses Eq. (A3) to determine the width, one finds $W^2=-\langle y\rangle_d$; not zero as the width must be. For this reason, in our determination of the width, we have used the expression

$$W^2=3\langle y^2\rangle_d-4\langle y\rangle_d^2+\langle y\rangle_d\approx\frac{w^2}{2}\ . \quad \text{(A9)}$$

We have shown that the leading term in this expression is directly related to the mean-square width of the density profile centered on the average interface position, h_0; furthermore, this expression is zero for a sharp interface, as it should be. It is this expression for the width that is used in studying the structure of the interfaces in the text of the paper. In earlier work on the first moment of the interface, we have used similar arguments to "correct" for short-time differences between the sum and integral evaluations of the moments, resulting in a shift of 1.3 in our time origin $t=1.3+m/L$. Both this "correction" to the time and the addition of $\langle y\rangle_d$ to the interfacial width in Eq. (A9) only affect the short-time behavior, serving to extend the asymptotic fractal scaling of the largest viscosity ratios to short times [see Fig. 3 of Ref. (18)].

[1] F. Family and T. Vicsek, *Dynamics of Fractal Surfaces* (World Scientific, Singapore, 1991).
[2] V. K. Horvath, F. Family, and T. Vicsek, J. Phys. A **24**, L25 (1991).
[3] M. A. Rubio, C. A. Edwards, A. Dougherty, and J. P. Gollub, Phys. Rev. Lett. **63**, 1685 (1989).
[4] S. He, G. Kahanda, and P.-Z. Wong, Phys. Rev. Lett. **69**, 3731 (1992).
[5] M. A. Cotta *et al.*, Phys. Rev. Lett. **70**, 4106 (1993).
[6] G. Kahanda and P.-Z. Wong, Phys. Rev. Lett. **68**, 3741 (1992).
[7] T. Vicsek, M. Cserzo, and V. K. Horvath, Physica A **167**, 315 (1990).
[8] S. V. Buldyrev *et al.*, Phys. Rev. A **45**, R8313 (1992).
[9] J. Zhang *et al.*, Physica A **189**, 383 (1992).
[10] C. S. Nolle, B. Koiller, N. Martys, and M. O. Robbins, Phys. Rev. Lett. **71**, 2074 (1993).
[11] M. Kardar, G. Parisi, and Y. C. Zhang, Phys. Rev. Lett. **56**, 889 (1986).
[12] Y.-C. Zhang, J. Phys. (France) **51**, 2129 (1990).
[13] V. K. Horvath, F. Family, and T. Vicsek, Phys. Rev. Lett. **67**, 3207 (1991).
[14] C.-H. Lam and L. M. Sander, Phys. Rev. E **48**, 979 (1993).
[15] K. Sneppen, Phys. Rev. Lett. **69**, 3539 (1992).
[16] D. A. Kessler, H. Levine, and Y. Tu. Phys. Rev. A **43**, 4551 (1991).
[17] K. J. Maloy, A. Hansen, E. L. Hinrichsen, and S. Roux, Phys. Rev. Lett. **68**, 213 (1992).
[18] M. Ferer, W. N. Sams, R. Geisbrecht, and D. H. Smith, Phys. Rev. Lett. E **47**, 2713 (1993). $\langle x\rangle$, the average position of the injected fluid, was characterized; here, $\langle h\rangle\approx 2\langle x\rangle$.
[19] M. Ferer, R. A. Geisbrecht, W. N. Sams, and D. H. Smith, Phys. Rev. A **45**, 6973 (1992).
[20] I. Fatt, Trans. Metall. Soc. AIME **207**, 144 (1956).
[21] R. Lenormand, E. Touboul, and C. Zarcone, J. Fluid Mech. **189**, 165 (1988).
[22] J.-D. Chen and D. Wilkinson, Phys. Rev. Lett. **55**, 1892 (1985).
[23] G. W. Thomas, *Principles of Hydrocarbon Reservoir Simulation* (International Human Resources Development Corporation, Boston, 1982).
[24] M. J. King and H. Scher, Phys. Rev. A **41**, 874 (1990).
[25] J. Kertesz and D. Wolf, J. Phys. A **21**, 747 (1988).